Published in final edited form as:
Nature. 2010 February 4; 463(7281): 657–661. doi:10.1038/nature08704.

Evidence for grid cells in a human memory network

Christian F. Doeller[1,2], **Caswell Barry**[1,3,4], and **Neil Burgess**[1,2]

[1]UCL Institute of Cognitive Neuroscience, University College London, London, United Kingdom

[2]UCL Institute of Neurology, University College London, London, United Kingdom

[3]UCL Department of Cell and Developmental Biology, University College London, London, United Kingdom

[4]UCL Institute of Behavioural Neuroscience, University College London, London, United Kingdom

Abstract

Grid cells in entorhinal cortex of freely-moving rats provide a strikingly periodic representation of self-location[1] which is suggestive of very specific computational mechanisms[2-4]. However, their existence in humans and distribution throughout the brain are unknown. Here we show that the preferred firing directions of directionally-modulated grid cells in rat entorhinal cortex are aligned with the grids, and that the spatial organization of grid cell firing is more strongly apparent at faster than slower running speeds. Since the grids are also aligned with each other[1,5], we predicted a macroscopic signal visible to functional magnetic resonance imaging (fMRI) in humans. We then looked for this signal as participants explored a virtual reality environment, mimicking the rats' foraging task: fMRI activation and adaptation showing a speed-modulated 6-fold rotational symmetry in running direction. The signal was found in a network of entorhinal/subicular, posterior and medial parietal, lateral temporal and medial prefrontal areas. The effect was strongest in right entorhinal cortex, and the coherence of the directional signal across entorhinal cortex correlated with spatial memory performance. Our study illustrates the potential power of combining single unit electrophysiology with fMRI in systems neuroscience. Our results provide the first evidence for grid-cell-like representations in humans, and implicate a specific type of neural representation in a network of regions which support spatial cognition and also, intriguingly, autobiographical memory.

Grid cells recorded in medial entorhinal cortex of freely moving rodents fire whenever the animal traverses the vertices of an equilateral triangular grid covering the environment (see Fig. 1a), and may provide a neural substrate for path integration[1-3,5,6]. However, it is not known whether or not grid cells exist in humans, or how widespread the network of neurons with grid-like firing is, although the pre- and para-subiculum[7] and posterior parietal cortex[8] have been implicated.

Could grid cell firing be detected in the functional magnetic resonance imaging (fMRI) signal, which reflects changes in metabolic activity across thousands of individual neurons[9]? The grid patterns of neighbouring cells are offset so as to 'tile' the environment[1], making

Correspondence and requests for materials should be addressed to C.F.D. (c.doeller@ucl.ac.uk), C.B. (caswell.barry@ucl.ac.uk) or N.B. (n.burgess@ucl.ac.uk)..

Supplementary Information is linked to the online version of the paper at www.nature.com/nature.

Author Contributions C.F.D., C.B. and N.B. jointly conceived and designed the experiments. C.F.D. performed the fMRI experiment and data analyses; C.B. performed the single-unit experiment and data analyses; N.B. gave direction on analyses; all authors discussed the analyses and results and contributed to the paper.

Author Information Reprints and permissions information is available at www.nature.com/reprints.

Europe PMC Funders Author Manuscripts

systematic variation in population activity with *position* unlikely. However, three factors may allow detection using fMRI. (i) The angular orientations of the grids relative to the environment appears to be constant across cells, whether they are neighbouring[1] or farther apart[5] (Supplementary Fig. 1), and rotate coherently when salient distal cues are rotated[1,6]. The other two factors result from new analyses presented here. (ii) The firing of 'conjunctive' grid cells, found in the deeper layers of entorhinal cortex[6] and in pre- and parasubiculum[7], is modulated by running direction[6]. Here we show that the directions of modulation of conjunctive grid cells are aligned with the main axes of the grids (Fig. 1a-c). These first two factors will create systematic differences in neural population dynamics for runs aligned or misaligned with the main axes of the grids (Fig. 2). (iii) A third factor is running speed: the rate[6] and inter-burst frequency[10] of grid cell firing and the frequency with which individual firing fields in a grid are sampled increase with running speed. In addition, we show that the spatial organisation of grid cell firing is more strongly apparent during fast running than during slow running and immobility (Fig. 1d; see Methods for details and Supplementary Figs. 2-6 for further analyses and recording locations). Thus entorhinal grid cells form a coherent population in which the common effects of orientation and speed of movement could produce a macroscopic signal visible with fMRI.

We recorded whole brain fMRI data while human participants navigated within a virtual reality (VR) arena, mimicking the foraging task in rodents, see Methods for details. The arena comprised a grassy plain bounded by a cylindrical cliff, containing a single intra-maze landmark and surrounded by a background scene providing orientation cues rendered at infinity (Fig. 2). Participants collected and replaced objects found within the arena. Memory was measured as the proximity of the replacement location to the correct location (Supplementary Fig. 7 and ref.[11]).

If orientationally-aligned grid cell firing is present, there should be an effect of running direction with 6-fold rotational symmetry, reflecting the differences between running aligned or misaligned to the grid axes, and this effect should be modulated by running speed (Fig. 2). We defined an anatomical region of interest (ROI) on the entorhinal cortices, and examined one half of the fMRI data for modulation by running direction and speed to find the orientation of potential grids within each participant's entorhinal cortex. Briefly, we used a quadrature filter to identify the orientation of any 6-peaked sinusoidal modulation of signal as a function of running direction: providing the potential grid orientation in each voxel (Supplementary Fig. 8 and Methods). The potential grid orientations were significantly clustered across voxels in the ROI in 34/42 participants (Rayleigh test, accounting for spatial smoothing, on each participant; $P<<0.00001$ for the population, Monte Carlo simulation; Supplementary Fig. 9). The mean grid orientation for the entorhinal ROI (φ) was defined as the population vector (vector sum of orientations weighted by amplitude), and calculated for data corresponding to fast, medium and slow runs.

We then examined the second half of the data for differential activation for fast, medium and slow runs aligned versus misaligned to each participant's mean grid orientation. We looked for sinusoidal modulation of activation with 6-fold rotational symmetry aligned with each participant's mean grid orientation across the *whole brain* (using the regressor $\cos(6[\theta(t)-\varphi])$ where $\theta(t)$ is running direction; Supplementary Fig. 8). We found a significant activation in the right entorhinal cortex for fast runs (Fig. 3a-b). Direct comparison of activation for fast runs aligned versus misaligned to each participant's mean grid orientation showed a similar effect (Fig. 3d). Similar sinusoidal modulations were present in left entorhinal cortex, although slightly less reliably than on the right, and in the mean response of the entorhinal ROI (Supplementary Fig. 10). No activation elsewhere in the brain reached the significance level for this whole-brain analysis. Equivalent analyses for medium or slow runs, or looking for 4- or 8-fold (Fig. 3b-c) or even 5- or 7-fold rotational symmetry (Supplementary Fig. 11)

failed to show significant activation. No significant activation was found when the analyses applied to the entorhinal ROI were performed to control ROIs in the posterior right hippocampal location associated with memory performance in this task[11] or the visual cortical location showing adaptation to running direction (below), see Supplementary Fig. 12. Supplementary figures 13-15 show control analyses of behaviour in rats and humans.

Consistent with grid cells, the mean grid orientations in the 6-fold symmetry model varied randomly *between participants*, ruling out a role for specific visual features of the environment (Supplementary Fig. 16). Interestingly, the coherence of the potential grid orientations in each participant's right entorhinal cortex was significantly correlated with that participant's spatial memory performance (Fig. 3f). This parallels findings that entorhinal cortex activation can predict memory performance[12,13], and provides a first indication that grid-like representations might usefully guide behaviour in mammals.

An independent indicator of variation in the dynamics of neuronal activity is provided by fMRI adaptation[14-17], i.e., reduced signal from activation of a representation that was recently active compared to a previously inactive one. During runs aligned with the grid, a smaller proportion of grid cells will fire but will do so at a higher rate, while more grid cells will be active during misaligned runs but at a lower rate (Supplementary Fig. 17). Given the complex non-linear dynamical relationship between neuronal activation and fMRI adaptation[9] we predicted that differences in the dynamics of neuronal activity when running aligned to the grids compared to misaligned would cause differences in fMRI adaptation, and that these differences would also vary with running speed.

We first checked whether the more basic effect of fMRI adaptation to running direction occurred within our virtual navigation paradigm. We made separate adaptation regressors (the logarithm of the time since last running in the current direction) for fast, medium and slow runs. We found significant adaptation to running direction in visual cortex extending into posterior parahippocampal/lingual and retrosplenial cortices, with larger effects for fast than for slow runs, see Fig. 4a-b. The adaptation effect is independent of variations in angular velocity (see Methods) and is consistent with adaptation to the background visual scene (which is rendered at infinity; viewing direction is the same as running direction), as previously found with static scenes in similar areas[14,16]. It is also consistent with view-specific single unit responses in humans[18] or with the presence of head-direction cells[19] which have been reported in retrosplenial cortex[20].

Given the robust fMRI adaptation to virtual running direction, we tested our specific prediction that adaptation in entorhinal cortex is modulated by running direction with 6-fold rotational symmetry and by running speed. Accordingly we looked for regions showing a reduction in fMRI signal according to how recently participants were running at 60° to the current direction which was greater for fast than for slow running. Unlike our analysis of whole brain activation as a function of mean grid orientation in the entorhinal ROI (Fig. 3), this analysis can be directly applied to the whole brain without reference to specific ROIs. As predicted, right entorhinal cortex (extending into subiculum) showed 60° shifted directional adaptation, independent of any effect of basic directional adaptation, as did regions in posterior parietal, lateral temporal and medial prefrontal cortices, see Fig. 4c. Medial parietal cortex also showed 60°shifted directional adaptation, in addition to the basic directional adaptation described above, consistent with the presence of both visual/head-direction and grid-like representations, see Supplementary Fig 18. The adaptation effect in all of these regions was strongly modulated by the participants' virtual running speed, being higher for fast compared to slow runs (Fig. 4d) and the effect was specific to 60° rather than 45° or 90° shifted directional adaptation (Fig. 4e).

Do these remote regions showing 60° shifted directional adaptation also show the sinusoidal modulation of activation seen in entorhinal cortex during fast running, consistent with the presence of grid-like representations in these regions too? We examined the mean response to the sinusoidal regressor defined in entorhinal cortex in 8mm-radius ROIs centred on the locations of peak adaptation. The responses in medial prefrontal (one-tailed t-test; P=0.008), medial parietal (P=0.002) and lateral temporal (left, P=0.019; right, P=0.0005) ROIs, but not the posterior parietal ROI (P=0.058), reached significance for this specific prediction. Overall, these results suggest a network of regions containing coherently aligned neural representations with 6-fold rotational symmetry, although the responses in remote regions were weaker than in right entorhinal cortex (e.g. not reaching significance in the initial whole-brain split-half analysis), possibly reflecting a lower concentration of grid-like cells.

Our results provide the first evidence that human entorhinal cortex encodes virtual movement direction with 6-fold symmetry, consistent with a coherently-oriented population of grid cells similar to those found in rat entorhinal cortex[1,5,6] and pre- and parasubiculum[7]. The dependence of directional modulation on running speed is consistent with the effects of speed on the firing rate[6,10] and apparent spatial organisation (Fig. 1d) of grid cells, while effects of speed on other aspects of behaviour may also contribute (see e.g., Supplementary Fig. 14). The relationship to spatial memory of the directional coherence of potential grids across entorhinal cortex provides a first indication that grid-like representations might usefully guide behaviour.

Because we can only measure effects of direction and speed (not location) in the fMRI signal, our findings could reflect the presence of grid cells, or movement-related responses from head-direction[19], or 'conjunctive' directional grid[6,7] cells, if they form coherent populations whose firing has 6-fold rotational symmetry. We showed that conjunctive grid cells from rat entorhinal cortex have such an organisation (Fig. 1). Our finding of similar and aligned fMRI responses from subicular, posterior/medial parietal, lateral temporal, and medial prefrontal cortices suggest that populations with similar properties also exist elsewhere, a prediction directly testable in rodents (see also refs.[7,8]). These results outline a circuit for navigation, consistent with suggestions that medial and lateral temporal, posterior and medial parietal and medial prefrontal areas cooperate to support spatial cognition[2,8,11,21,22], and implicate a specific type of underlying neural representation.

Our study illustrates the ability to infer neural representations in humans by using fMRI in conjunction with single unit recording in behaving animals, promising a coherent understanding of behaviour at the neural and systems levels. The observed grid-like representations support spatial memory (Fig. 3f) and are found in a circuit of regions which strikingly overlaps the network for autobiographical memory and imagery, e.g. refs.[21,23,24]. These types of regularly repeating representation may provide a clue to the neural basis of autobiographical memory, perhaps encoding temporal as well as spatial context[3,4,25-27] for combination with parallel networks representing non-spatial information[25,28-30].

Methods Summary

Single unit recording experiment in rats

Single unit recordings were made from the medial entorhinal cortex of 17 male, Lister hooded rats, in accordance with appropriate Home Office Project and Personal licences. Each animal received a single microdrive carrying four tetrodes. While animals foraged for sweetened rice in a familiar environment, their positions and concomitant action potentials were captured using a standard procedure[5]. Grid cells were identified on the basis of their hexagonal spatial firing pattern, the regularity of which was assessed using a gridness measure[1,5]. Post-recording animals were sacrificed, perfused with phosphate buffered saline

and then with 4% paraformaldehyde. Histology was conducted to confirm recording locations. See methods and ref.[5] for details.

Functional neuroimaging experiment in humans

Forty-two male participants took part in this experiment (aged 18-31, mean age 23.1 years). The study was approved by the local Research Ethics Committee. Functional images were acquired on a 3T Siemens Allegra scanner using a gradient-echo EPI pulse sequence. Imaging data were analyzed with SPM5 (www.fil.ion.ucl.ac.uk/spm/), including standard preprocessing procedures (spatial realignment, correction for differences in slice acquisition time, spatial normalization and smoothing) and modelling the data by a set of general linear models. During the virtual reality task, participants were presented with a first-person perspective of a grassy plane surrounded by a circular cliff. Participants moved the viewpoint by using their right hand to operate keys to move forward and turn left or right. Throughout the experiment, participants collected and replaced everyday objects within the arena. See methods and ref.[11] for details.

Supplementary Material

Refer to Web version on PubMed Central for supplementary material.

Acknowledgments

We gratefully acknowledge K. Jeffery and J. O'Keefe for providing help and facilities for single unit recording, the Wellcome Trust Centre for Neuroimaging for providing help and scanning facilities, J. Krupic and R. Hayman for help with single unit data collection, A. Jeewajee for help with analyses, J. King for help with VR programming, and useful discussions with P. Dayan, K. Friston, U. Frith, C. Hall, A. Jeewajee, J. O'Keefe and M. Witter. This work was funded by the UK Medical Research Council and the European Union (SpaceBrain grant).

References

1. Hafting T, Fyhn M, Molden S, Moser MB, Moser EI. Microstructure of a spatial map in the entorhinal cortex. Nature. 2005; 436:801–806. [PubMed: 15965463]
2. McNaughton BL, Battaglia FP, Jensen O, Moser EI, Moser MB. Path integration and the neural basis of the 'cognitive map'. Nat. Rev. Neurosci. 2006; 7:663–678. [PubMed: 16858394]
3. Burgess N, Barry C, O'Keefe J. An oscillatory interference model of grid cell firing. Hippocampus. 2007; 17:801–812. [PubMed: 17598147]
4. Hasselmo ME. A model of episodic memory: mental time travel along encoded trajectories using grid cells. Neurobiol. Learn. Mem. 2009; 92:559–573. [PubMed: 19615456]
5. Barry C, Hayman R, Burgess N, Jeffery KJ. Experience-dependent rescaling of entorhinal grids. Nat. Neurosci. 2007; 10:682–684. [PubMed: 17486102]
6. Sargolini F, et al. Conjunctive representation of position, direction, and velocity in entorhinal cortex. Science. 2006; 312:758–762. [PubMed: 16675704]
7. Boccara CN, et al. Grid cells in presubiculum and parasubiculum. FENS Abstr. 2008; vol.4 128.21.
8. Whitlock JR, Sutherland RJ, Witter MP, Moser MB, Moser EI. Navigating from hippocampus to parietal cortex. Proc. Natl. Acad. Sci. U. S. A. 2008; 105:14755–14762. [PubMed: 18812502]
9. Logothetis NK. What we can do and what we cannot do with fMRI. Nature. 2008; 453:869–878. [PubMed: 18548064]
10. Jeewajee A, Barry C, O'Keefe J, Burgess N. Grid cells and theta as oscillatory interference: electrophysiological data from freely moving rats. Hippocampus. 2008; 18:1175–1185. [PubMed: 19021251]
11. Doeller CF, King JA, Burgess N. Parallel striatal and hippocampal systems for landmarks and boundaries in spatial memory. Proc. Natl. Acad. Sci. U. S. A. 2008; 105:5915–5920. [PubMed: 18408152]

12. Fernandez G, Brewer JB, Zhao Z, Glover GH, Gabrieli JD. Level of sustained entorhinal activity at study correlates with subsequent cued-recall performance: a functional magnetic resonance imaging study with high acquisition rate. Hippocampus. 1999; 9:35–44. [PubMed: 10088898]
13. Olsen RK, et al. Performance-related sustained and anticipatory activity in human medial temporal lobe during delayed match-to-sample. J. Neurosci. 2009; 29:11880–11890. [PubMed: 19776274]
14. Epstein R, Graham KS, Downing PE. Viewpoint-specific scene representations in human parahippocampal cortex. Neuron. 2003; 37:865–876. [PubMed: 12628176]
15. Grill-Spector K, Henson R, Martin A. Repetition and the brain: neural models of stimulus-specific effects. Trends Cogn Sci. 2006; 10:14–23. [PubMed: 16321563]
16. Park S, Intraub H, Yi DJ, Widders D, Chun MM. Beyond the edges of a view: boundary extension in human scene-selective visual cortex. Neuron. 2007; 54:335–342. [PubMed: 17442252]
17. Bakker A, Kirwan CB, Miller M, Stark CE. Pattern separation in the human hippocampal CA3 and dentate gyrus. Science. 2008; 319:1640–1642. [PubMed: 18356518]
18. Ekstrom AD, et al. Cellular networks underlying human spatial navigation. Nature. 2003; 425:184–188. [PubMed: 12968182]
19. Taube JS. Head direction cells and the neuropsychological basis for a sense of direction. Prog. Neurobiol. 1998; 55:225–256. [PubMed: 9643555]
20. Chen LL, Lin LH, Green EJ, Barnes CA, McNaughton BL. Head-direction cells in the rat posterior cortex. I. Anatomical distribution and behavioral modulation. Exp. Brain Res. 1994; 101:8–23. [PubMed: 7843305]
21. Byrne P, Becker S, Burgess N. Remembering the past and imagining the future: a neural model of spatial memory and imagery. Psychol Rev. 2007; 114:340–375. [PubMed: 17500630]
22. Wolbers T, Wiener JM, Mallot HA, Buchel C. Differential recruitment of the hippocampus, medial prefrontal cortex, and the human motion complex during path integration in humans. J Neurosci. 2007; 27:9408–9416. [PubMed: 17728454]
23. Maguire EA. Neuroimaging studies of autobiographical event memory. Philos. Trans. R. Soc. Lond B Biol. Sci. 2001; 356:1441–1451. [PubMed: 11571035]
24. Schacter DL, Addis DR, Buckner RL. Remembering the past to imagine the future: the prospective brain. Nat. Rev. Neurosci. 2007; 8:657–661. [PubMed: 17700624]
25. O'Keefe, J.; Nadel, L. The hippocampus as a cognitive map. Oxford University Press; 1978.
26. Howard MW, Fotedar MS, Datey AV, Hasselmo ME. The Temporal Context Model in spatial navigation and relational learning: Toward a common explanation of medial temporal lobe function across domains. Psychol. Rev. 2005; 112:75–116. [PubMed: 15631589]
27. Pastalkova E, Itskov V, Amarasingham A, Buzsaki G. Internally generated cell assembly sequences in the rat hippocampus. Science. 2008; 321:1322–1327. [PubMed: 18772431]
28. Gaffan D. Scene-specific memory for objects: a model of episodic memory impairment in monkeys with fornix transection. J. Cogn Neurosci. 1994; 6:305–320.
29. Knierim JJ. Neural representations of location outside the hippocampus. Learn. Mem. 2006; 13:405–415. [PubMed: 16882858]
30. Eichenbaum H, Yonelinas AP, Ranganath C. The medial temporal lobe and recognition memory. Annu. Rev. Neurosci. 2007; 30:123–152. [PubMed: 17417939]

Europe PMC Funders Author Manuscripts

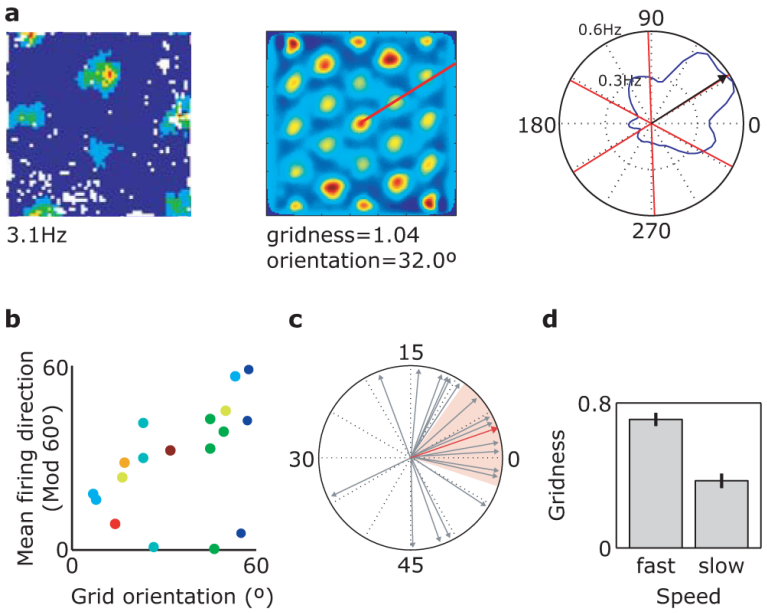

Figure 1. The mean firing directions of directional grid cells are aligned with the grid

a, Left – Firing rate map of a typical 'conjunctive' directional grid cell showing firing rate as a function of the rat's location within a $1m^2$ box (red: high firing rate, blue: low rate; white: unvisited location). Centre – Spatial autocorrelogram constructed from the ratemap. Right – Polar firing rate map for the same cell. Black arrow indicates mean firing direction. Red lines indicate the main axes of the grid firing pattern identified from the spatial autocorrelogram (see centre). **b,** Scatter plot of all directional grid cells (n=18) showing grid orientation vs. circular mean firing direction, modulo 60°. Cells from different rats (n=8) are coloured differently. **c,** Angular difference between the circular mean firing direction of each cell and the nearest axis of its grid-like firing pattern is not distributed uniformly (Rayleigh test of uniformity; P=0.007) and is significantly clustered around zero (Monte Carlo simulation; P<0.001). Red arrow shows the mean difference (3.15°), red shaded area indicates the 95% confidence interval. **d,** The spatial organization of grid cell firing is less strongly apparent during slow movement and immobility than during fast movement. Bar graph showing mean gridness (a measure of 6-fold spatial periodicity, see Methods) score for 113 grid cells, separately for fast and slow movements (median split), paired t-test; $P=2.2\times10^{-11}$.

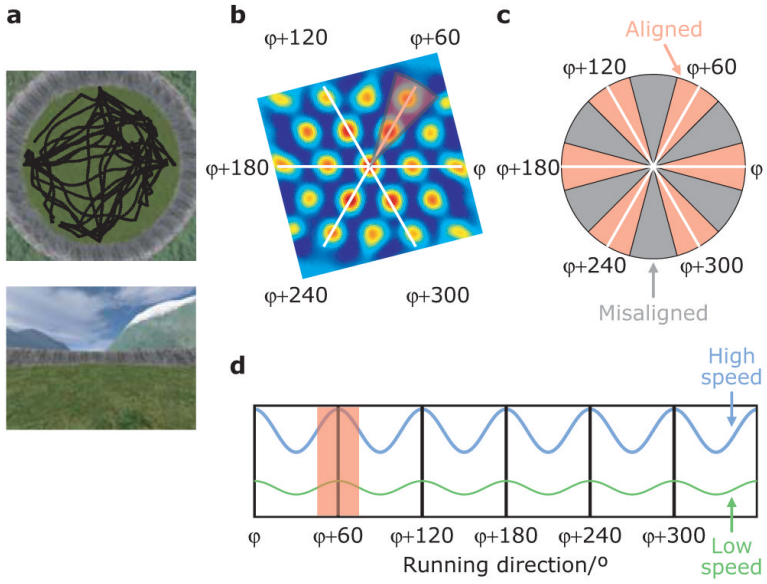

Figure 2. fMRI: virtual reality arena and experimental logic

a, Human participants (n=42) explored a circular virtual reality environment, bounded by a cliff and surrounded by orientation cues (mountains), finding objects and having to replace them in the correct locations. Above: aerial view, including one participant's virtual trajectory (black line). Below: participant's view. **b,** Spatial autocorrelogram of a typical grid cell showing the three main axes of the grid (white lines) and a 30° sector aligned with the grid (red). **c,** Schematic of running directions aligned (red) and misaligned (grey) with the grid. **d,** Given the alignment of directionally modulated grid cells with the grid and the constant grid orientation across cells (Fig. 1b), we predicted a sinusoidal modulation of fMRI signal by running direction with 6-fold rotational symmetry, and a stronger effect for faster (blue) than slower (green) runs (see Fig. 1d). Note that the absolute orientation of the pattern ('mean grid orientation', φ) will not be known *a priori*.

Europe PMC Funders Author Manuscripts

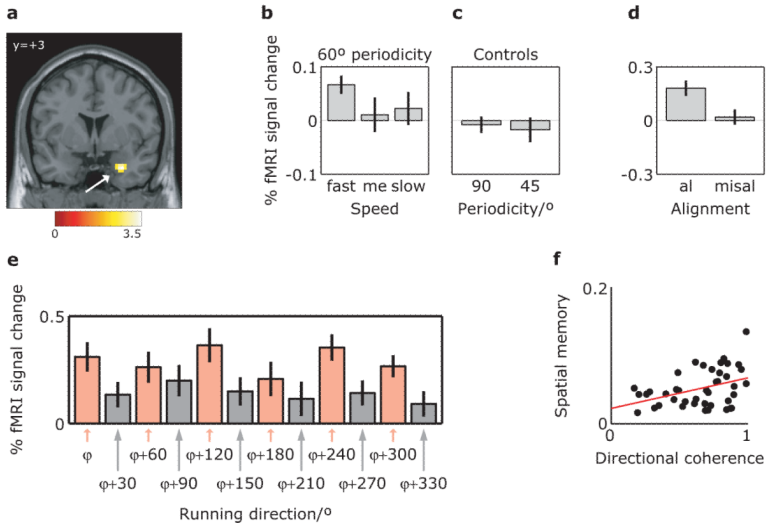

Figure 3. Modulation of entorhinal cortical activity by running direction with 6-fold rotational symmetry, and correlation with spatial memory

a, Sinusoidal modulation of activity by running direction with 6-fold rotational symmetry. The orientation of potential grids in each participant's entorhinal cortex was estimated on one half of the data, and the correspondingly aligned sinusoidal regressor was fitted to the other half of the data, showing a significant modulation only in right entorhinal cortex. Plot shows fMRI activation for fast runs on an aligned structural template; colorbar indicates *t*-statistic; all reported effects of whole-brain analyses are significant at $P<0.001$ uncorrected; the *t*-image is thresholded at $P<0.01$ for display purposes; peak MNI coordinates: 30/3/−30; peak z-score=3.59. **b,** Directional modulation depends on running speed, being present for fast, but not for medium or slow runs. **c,** Directional modulation during fast runs has 60° directional periodicity, not 90° or 45° (i.e. to 6-fold rather than 4- or 8-fold rotational symmetry). Bar plots in (b) and (c) show the mean amplitude of sinusoidal modulation for the peak voxel in (a). **d,** Activation for aligned (within 15° of the main axes of the grid, see Fig. 2c) and misaligned fast runs relative to baseline (epochs of no movement in the environment) in the peak voxel shown in (a), confirming the sinusoidal modulation effect. **e,** To examine the pattern underlying these effects, we plotted the average fMRI signal over the entire timeseries of all voxels in the entorhinal ROI for all directions of aligned (red) and misaligned (grey) fast runs, relative to baseline, see Fig. 2c. **f,** The coherence of the potential grid orientations in each participant's right entorhinal cortex (mean length of resultant direction vector) correlated significantly with that participant's spatial memory (1/mean distance of object replacement locations from correct locations; range = 7.4 to 61.7 virtual meters; mean=25.4, Spearman's rho=0.32, $P=0.039$. Each dot represents one participant. me, medium speed; al, aligned runs; misal, misaligned runs; vm, virtual metres. Bars here and in other figures show mean and s.e.m. over participants.

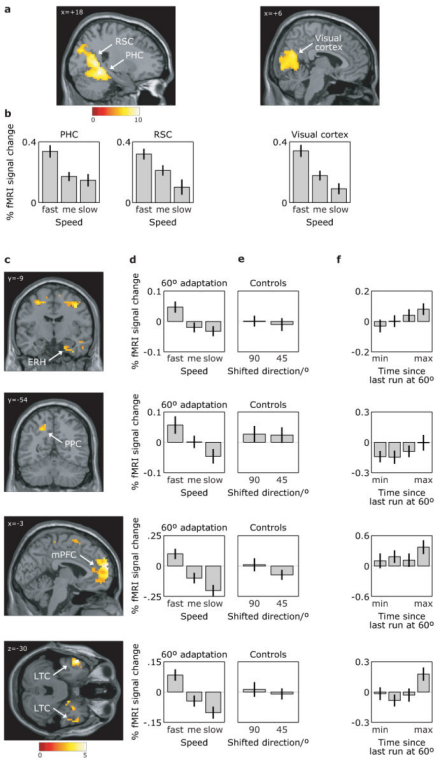

Figure 4. fMRI adaptation to running direction and to runs at 60° from it

a, Activity in parahippocampal (PHC; 24/−48/−12; z=7.13), retrosplenial (RSC; 18/−57/18; z=7.16), and visual (peak at 18/−69/15; z=7.11) cortices shows adaptation to absolute running direction. Plot shows the *t*-statistic for the parameter estimate of the adaptation regressor (log(time since last run in current direction)). **b,** Adaptation is greater for faster runs, showing the adaptation effect for the peak voxels in the three regions for fast, medium, and slow runs. **c,** fMRI adaptation to runs at 60° from the current direction (regressor: log(time since last run at 60° from the current direction)) is seen in a network of regions, including: entorhinal cortex extending into subiculum (ERH; 21/−9/−30; z=3.28), anterior entorhinal/perirhinal (33/0/−27; z=3.69); posterior parietal (PPC; −18/−54/45; z=3.24); medial prefrontal (mPFC; −3/63/15; z=4.96), lateral temporal cortices (LTC; left: −54/9/−30; z=4.99; right: 42/15/−36; z=3.48) and precentral gyrus/superior frontal gyrus/ motor cortex. These effects are independent of any basic (360°) directional adaptation (images are exclusively masked by the effects of basic directional adaptation at threshold $P<0.05$, uncorrected). **d,** The 60° adaptation effect is specific to fast runs. **e,** No significant adaptation is seen for fast running at 45° or 90° from the current direction. **f,** fMRI activity as a function of time since last fast run at 60° from the current direction (log(time) binned in quartiles), illustrating the adaptation effect. Signal in (**d**)-(**f**) shown for the peak voxel in (**c**). All effects significant at $P<0.001$, uncorrected; For display purposes, *t*-images are thresholded at $P<0.000001$ in (**a**) and $P<0.01$ in (**c**).

Europe PMC Funders Author Manuscripts